Magnesium Technology 2012
Edited by: Suveen N. Mathaudhu, Wim H. Sillekens, Neale R. Neelameggham, and Norbert Hort
TMS (The Minerals, Metals & Materials Society), 2012

INTERMETALLIC PHASE FORMATION AND GROWTH IN THE MG-Y SYSTEM

K. Bermudez, S. Brennan, Y.H. Sohn

University of Central Florida, Advanced Materials Processing and Analysis Center

Department of Mechanical, Materials and Aerospace Engineering, Orlando, FL 32816, USA

Abstract

Rare earths have been added to magnesium alloys in order to improve the creep resistance, corrosion resistance and strength. Solid-to-solid diffusion couples were assembled between Mg (99.9%) and Y (99.9%) to investigate the formation and growth of intermetallic phases and interdiffusion in the Mg-Y system. The diffusion anneals were performed at 450, 500 and 550°C for 360, 240 and 120 hours, respectively. The intermetallic layers that developed were the δ-Mg_2Y and ε-$Mg_{24}Y_5$ phases, however the MgY phase did not form. A substantial penetration of Y in Mg was observed, however along with Kirkendall porosity that indicates faster diffusion of Mg than Y in Mg solid solution. The activation energies for parabolic growth in ε-$Mg_{24}Y_5$ and δ-Mg_2Y were calculated to be 84 kJ/mol and 77 kJ/mol, respectively.

Keywords: Magnesium, Yttrium, in ε-$Mg_{24}Y_5$ and δ-Mg_2Y

Introduction

The increasing use of lightweight magnesium (Mg) alloys in aerospace and transportation applications has led the desire for more fundamental materials research in Mg-based systems. Rare earth elements (RE) have been found to improve the mechanical properties of magnesium at both room and high temperatures [1-3]. Yttrium (Y) additions enhance creep resistance and high temperature performance. In this study, solid-to-solid diffusion couples were used to observe the phase layer formation and growth within the binary Mg-Y system. Parabolic growth constants were calculated from measured phase layer thicknesses. The activation energies for growth were determined for the intermediate phase layers that were observed.

Analytical Framework and Experimental Procedure

The parabolic growth rate of a phase, k_p, can be described by:

$$k_p=\frac{Y^2}{t} \quad (1)$$

where Y is the phase layer thickness and t is the annealing time. Typically, this follows an Arrhenius temperature dependence given as:

$$k_p=k_o\exp\left[-\frac{Q_k}{RT}\right] \quad (2)$$

where k_o is the pre-exponential factor and Q_k is the activation energy for growth. R is the universal gas constant (8.314 kJ/mole-K) and T is the absolute temperature (K).

Rods of pure Mg (99.9%) and pure Y (99.9%) were supplied from Alfa Aesar™ and sectioned into disks, approximately 3 mm thick. The diameter of each Mg disk was 7.9 mm and that of Y was 12.7 mm. All disks were metallographically polished down to 1 μm using non-oxidizing lubricants, and contact with water was avoided during the entire preparation stage. The prepared disks were assembled in between two inert alumina spacer disks and clamped in a stainless steel jig as shown in Figure 1.

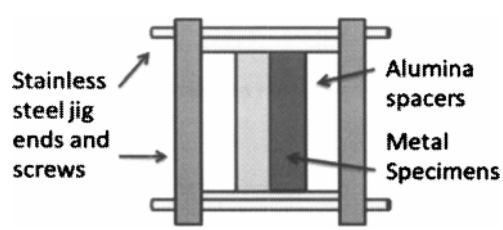

Figure 1: A schematic of the diffusion couple assembly in a stainless steel jig.

The diffusion couple jig assembly was then placed in a quartz capsule that was repeatedly evacuated to approximately 10^{-6} Torr and flushed with hydrogen and ultra-high purity argon at least three times, then backfilled with ultra-high purity Ar to a pressure that would be slightly above 1 atm at the respective annealing temperature. The sealed capsule was then placed in a preheated furnace that was monitored with an independent type-K thermocouple and maintained within ±2° of the desired annealing temperature. The annealing times and temperatures were 450, 500, and 550°C for 360, 240 and 120 hours, respectively. After the anneal, the capsule was quickly removed and quenched in water at room

temperature. The full jig assembly was mounted in epoxy and then cross-sectioned in a low speed saw with a diamond wafering blade. The cross-sections were then metallographically prepared and examined in an optical microscope to check the quality of the diffusion bond. Field emission scanning electron microscope (Zeiss™ Ultra-55 FE-SEM) was used to further examine the diffusion couple. and identify the phases present using X-ray energy dispersive spectroscopy (XEDS). Concentration profiles are also acquired across the interdiffusion zone by using electron microprobe analysis (EPMA) with a point to point scan using a step size of 5 μm and accelerating voltage of 20 keV. Pure standards of Mg and Y, present at the terminal ends of each diffusion couple were used along with ZAF correction for the determination of concentration profiles.

Results and Discussion

FE-SEM equipped with XEDS was initially employed to obtain backscatter electron micrographs of the interdiffusion zone, and identify each phase present in the diffusion couple according to the Mg-Y equilibrium binary phase diagram presented in Figure 2.

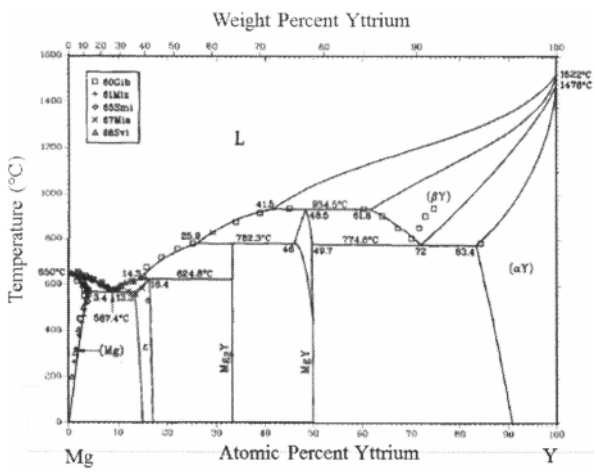

Figure 2: Mg-Y equilibrium binary phase diagram [4].

Two intermetallic phases were observed in all three diffusion couples: the ε-$Mg_{24}Y_5$ and δ-Mg_2Y phases as shown in the backscatter electron micrographs in Figure 3. These same two phases were also identified in the diffusion couple study by Zhao *et* al. [5]. The MgY phase was not observed in any of the diffusion couples examined in this study. In each diffusion couple, there were some cracks across the diffusion zone, most likely attributed to molar volume differences and quenching. Rectangular shaped pores were evident in all three couples in the Mg solid solution. These are Kirkendall pores that indicate the large intrinsic difference in diffusion of Mg: Mg atoms out of the Mg solid solution vs. Y atoms out the δ-phase and into the Mg solid solution.

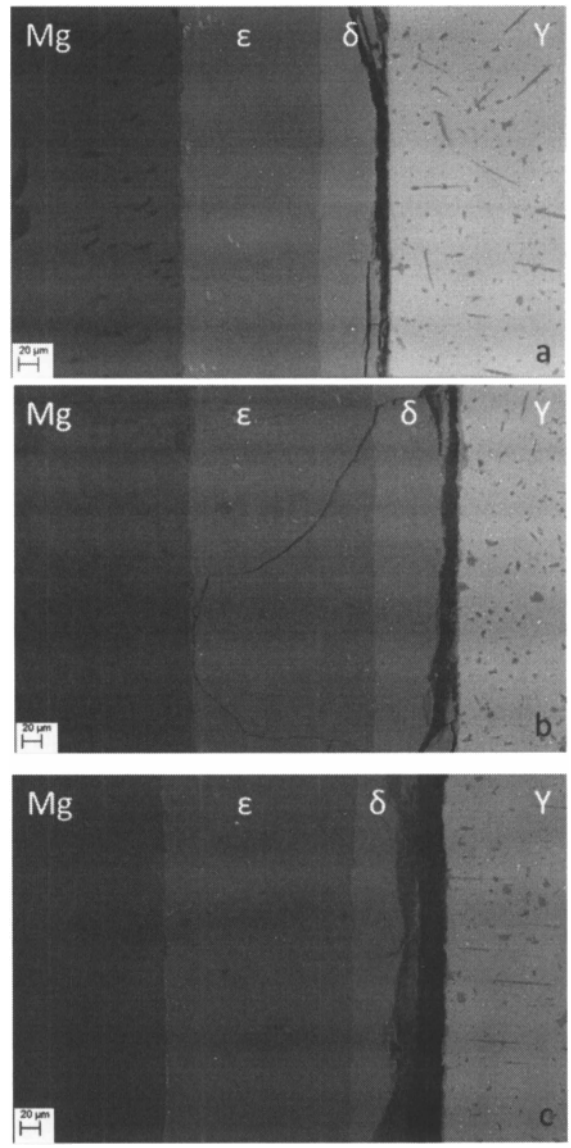

Figure 3: Backscatter electron micrographs from Mg-Y binary diffusion annealed at (a) 450°C for 360 hours, (b) 500°C for 240 hours and (c) 550°C for 120 hours.

EPMA (JEOL™ 733 SuperProbe) was employed to collect concentration profiles of Mg and Y across the cross section of each diffusion couple as presented in Figure 4. There is a significant solubility for Y in Mg in accordance to the equilibrium phase diagram. However, there is little to no solubility for Mg in Y, in contrast to the equilibrium phase diagram. Both intermetallic phases also exhibited some range of solubility, which was expected for the ε-phase, but not so for the Mg_2Y phase. In the equilibrium binary phase diagram, Mg_2Y is a line compound. In the study by Zhao *et* al. [5], solubility in both intermetallic phases was also observed, and an adjustment to the equilibrium phase diagram was proposed. A comparison of the solubility found by Zhao *et* al. [5] and the results of this study by EPMA are reported in Tables I and II, respectively, for ε-$Mg_{24}Y_5$ and δ-Mg_2Y. Similar ranges were found for the

two intermetallic phases developed in the Mg-Y binary system. The results of this study support the notion of adjusting the equilibrium phase diagram. Relevant coefficient of interdiffusion for Mg, ε-$Mg_{24}Y_5$ and δ-Mg_2Y will be reported elsewhere with due respect for uncertainty in concentration gradients and variation in molar volume.

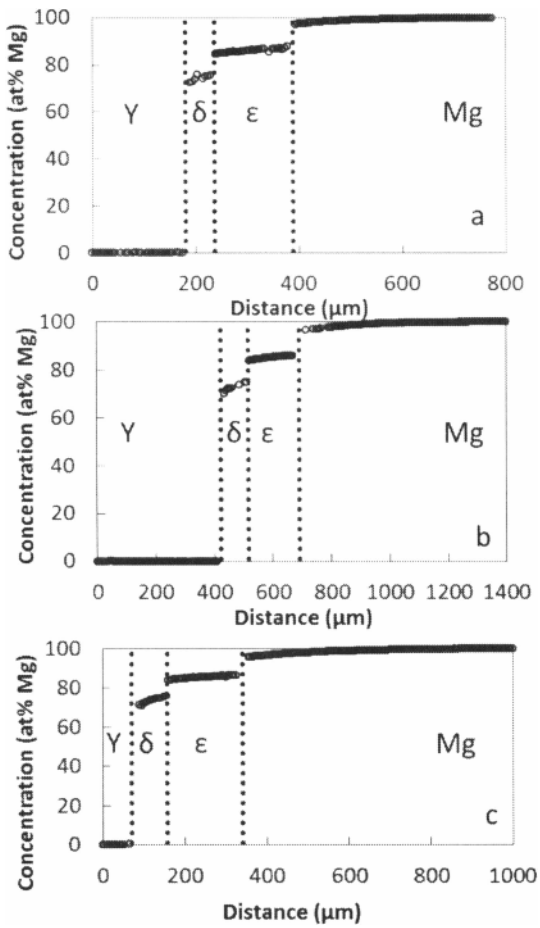

Figure 4: Concentration profiles of Mg and Y determined by EPMA from solid-to-solid diffusion couples annealed at (a) 450°C for 360 hours, (b) 500°C for 240 hours, and (c) 550°C for 120 hours.

Table I. Comparison of the Mg solubility limits in ε-$Mg_{24}Y_5$.

Temperature (°C)	Equilibrium Compositions of ε-$Mg_{24}Y_5$ phase boundaries (at.% Mg)			
	This Study		Zhao *et* al. [5]	
	Mg/ε	ε/δ	Mg/ε	ε/δ
400	N/A		88.0	84.2
450	88.0	84.7	88.1	84.4
500	86.1	84.0	88.1	84.9
550	86.6	84.0	N/A	

Table II. Comparison of the Mg solubility limits of δ-Mg_2Y.

Temperature (°C)	Equilibrium Compositions of δ-Mg_2Yphase boundaries (at.% Mg)			
	Current Study		Zhao et al. [5]	
	ε/δ	δ/Y	ε/δ	δ/Y
400	N/A		75.8	70.5
450	75.6	72.5	75.5	69.0
500	75.0	70.0	76.4	69.4
550	76.1	71.1	N/A	

Phase layer thickness measurements were made from backscatter electron micrographs for each diffusion couple, and parabolic growth constants were calculated using Eq. (1). The temperature dependence of the growth constants was determined using Eq. (2), and the activation energies of growth for both the ε-$Mg_{24}Y_5$ and δ-Mg_2Y phases were calculated from the Arrhenius plot presented in Figure 5. The measured layer thicknesses, pre-exponential factors and activation energies for growth are reported in Table III.

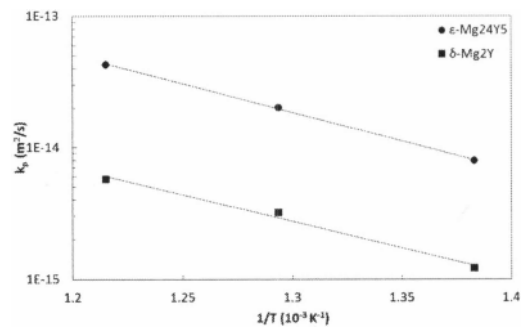

Figure 5: Temperature dependent growth constants for δ-Mg_2Y and ε-$Mg_{24}Y_5$.

The two intermetallic phases have activation energies that are close in magnitude, however, the thickness difference of each phase is apparently influenced by the pre-exponential factor, and suggests that the detailed mechanism of diffusion in δ-Mg_2Y and ε-$Mg_{24}Y_5$ phases may be very different.

Summary

Solid-to-solid binary diffusion couples between Mg and Y were assembled and annealed for 450, 500 and 550°C for 360, 240, and 120 hours respectively. SEM equipped with XEDS was used to identify the intermetallic phases that formed and grew, namely, the ε-$Mg_{24}Y_5$ and δ-Mg_2Y phases. However, the MgY phase was not observed in any of the diffusion couples. The pre-exponential factor and activation energies for the two intermetallic phases were calculated. The activation energy for ε-$Mg_{24}Y_5$ and δ-Mg_2Y were 84 and 77 kJ/mol, respectively. Despite the similar activation energies, the ε-$Mg_{24}Y_5$ phase was significantly larger than the δ-Mg_2Y phase, owing to a larger pre-exponential factor.

Table III. Activation energy and the pre-exponential factor of the parabolic growth constants for ε-$Mg_{24}Y_5$ and δ-Mg_2Y phases determined based on thickness measurements.

Parameters	Phase	550°C 120 h	500°C 240 h	450°C 360 h
Y (μm)	δ-Mg_2Y	70.5 (1.7)	74.4 (2.3)	56.1 (4.0)
	ε-$Mg_{24}Y_5$	192.6 (1.3)	186.7 (2.7)	143.4 (4.5)
k_o (m^2/s)	δ-Mg_2Y	4.89×10^{-10}		
	ε-$Mg_{24}Y_5$	8.84×10^{-9}		
Q_k (kJ/mol)	δ-Mg_2Y	77.3		
	ε-$Mg_{24}Y_5$	83.6		

Note: values in parenthesis are standard deviation.

Acknowledgments

The authors would like to thank the Material Characterization Facility at the University of Central Florida for the use of its equipment and the assistants of its technicians.

References

[1] M. Suzuki, H. Sato, K. Maruyama, H. Oikawa, *Mater. Sci. Eng. A* 252 (1998) 248-255.

[2] A. Tharumarajah, P. Koltun, *Journal of Cleaner Production* 15 (2007) 1007-1013.

[3] L. Gao, R. S. Chen, E. H. Han, *J. Alloy Compd.* 472 (2009) 234-240.

[4] H. Okamoto, "Mg-Y (Magnesium-Yttrium)," *Journal of Phase Equilibria*, 13, 1992, 105.

[5] H. Zhao, G. Qin, Y. Ren, W. Pei, D. Chen, Y. Guo, *J. Alloy Compd.* 509 (2011) 627-631